Subleading contributions to the chiral three-nucleon force. II. Short-range terms and relativistic corrections

V. Bernard,[1,*] E. Epelbaum,[2,†] H. Krebs,[2,‡] and Ulf-G. Meißner[3,4,§]

[1]*Institut de Physique Nucléaire, CNRS/Univ. Paris-Sud 11, (UMR 8608), F-91406 Orsay Cedex, France*

[2]*Institut für Theoretische Physik II, Ruhr-Universität Bochum, D-44780 Bochum, Germany*

[3]*Universität Bonn, Helmholtz-Institut für Strahlen- und Kernphysik (Theorie) and Bethe Center for Theoretical Physics, D-53115 Bonn, Germany*

[4]*Forschungszentrum Jülich, Institut für Kernphysik (IKP-3), Insitute for Advanced Simulation (IAS-4) and Jülich Center for Hadron Physics, D-52425 Jülich, Germany*

(Received 29 August 2011; published 1 November 2011)

We derive the short-range contributions and the leading relativistic corrections to the three-nucleon force at next-to-next-to-next-to-leading order in the chiral expansion.

DOI: 10.1103/PhysRevC.84.054001 PACS number(s): 13.75.Cs, 21.30.−x

I. INTRODUCTION

Chiral effective field theory allows for a consistent calculation of forces between two, three, and more nucleons (for recent reviews, see Refs. [1–3]). In this paper, we fill in the last missing part of the nuclear forces calculated at next-to-next-to-next-to-leading order (N^3LO) in the chiral expansion; namely, the short-range contributions and the leading relativistic corrections to the three-nucleon force (3NF). At this order, the 3NF is given by five topologies as shown in Ref. [4]. Three of these do not involve multinucleon operators and thus contribute at long range $r \sim 1/M_\pi$ and $r \sim 1/(2M_\pi)$, with M_π being the pion mass. The corresponding momentum and coordinate-space representations are given in that paper (see also [5]). Here, we work out the remaining terms corresponding to the two topologies involving four-nucleon operators (the short-range terms) as well as the relativistic $(1/m)$ corrections to the leading one- and two-pion exchange corrections. These appear at next-to-next-to-leading order (N^2LO). Throughout, m denotes the nucleon mass. Special care has to be taken to calculate these corrections consistently with the ones contributing to the two-nucleon force. With the formalism given here, one is now in the position to perform calculations in three (or more) nucleon systems consistently at N^3LO. It is important to stress that the 3NF at this order does not involve any new and unknown low-energy constants (LECs)—the full 3NF to this order thus depends just on two LECs, commonly called D and E, that parametrize the leading one-pion-contact term topology and the six-nucleon contact term at N^2LO. Note that an exploratory study of the effects of the long-range parts of the 3NF at N^3LO in the triton was recently presented in [6].

Our manuscript is organized as follows: In Sec. II we discuss the contributions of the one-pion-exchange-contact topology. Section III describes the calculation of the two-pion-exchange-contact topology while Sec. IV is devoted to the analysis of the leading relativistic corrections that also appear at N^3LO. We end with a brief summary and outlook. For the sake of completeness, in Appendix A we give the formal algebraic structure of the parts of the nuclear Hamiltonian which are relevant for our work. Finally, Appendix B contains the coordinate-space representation of the obtained results.

II. ONE-PION-EXCHANGE-CONTACT TOPOLOGY

We begin with the discussion of the one-pion-exchange contributions involving short-range contact interactions between two nucleons, which are shown in Fig. 1. It is important to keep in mind that these diagrams do not correspond to Feynman graphs. Rather, they schematically represent various contributions to the connected, irreducible part of the three-nucleon amplitude which gives rise to the three-nucleon force. Each diagram is to be understood as a set of all possible time-ordered-like graphs of the same topology (i.e., the same sequence of vertices). The precise meaning of the diagrams and their contributions to the nuclear Hamiltonian depend, strictly speaking, on the approach used to extract the irreducible part of the amplitude.[1] In this work, we adopt the method of unitary transformation which was already successfully applied to the derivation of nuclear forces Ref. [7–11] and more recently electromagnetic nuclear exchange current and charge operators [12,13]. It is also the same method that we used in Ref. [4] to compute the long-range parts of the 3NF at N^3LO. The resulting two- and many-body forces as well as the exchange currents are thus derived in the same theoretical approach from the effective chiral Lagrangian and are, per construction, consistent with each other.

Before discussing the results for individual diagrams we first outline the way the actual calculation is carried out. Starting from the effective chiral Lagrangian for pions and nucleons, we first compute the corresponding Hamilton density using the canonical formalism; see [14] for more

*bernard@ipno.in2p3.fr
†evgeny.epelbaum@rub.de
‡hkrebs@itkp.uni-bonn.de
§meissner@itkp.uni-bonn.de; www.itkp.uni-bonn.de/∼meissner/

[1]We remind the reader that nuclear potentials do not correspond to observable quantities and are, in general, scheme dependent.

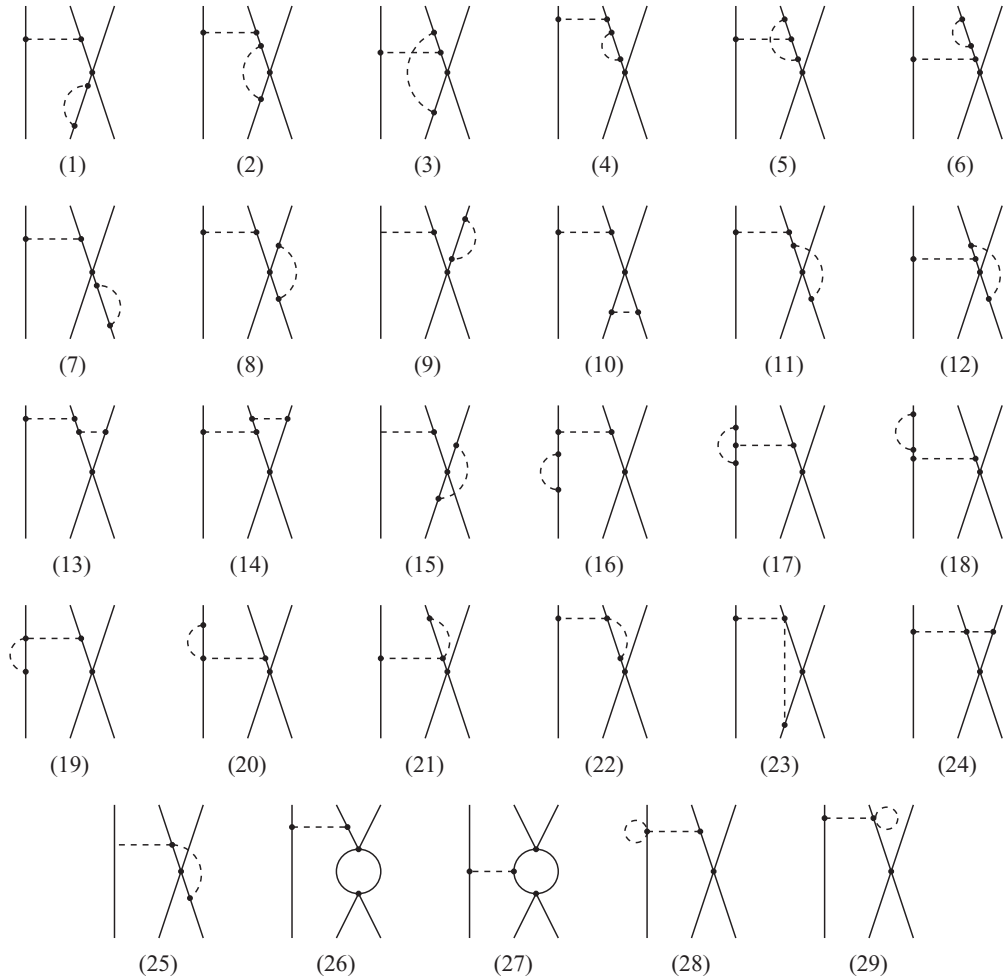

FIG. 1. Diagrams contributing to the one-pion-exchange-contact 3NF. Solid and dashed lines represent nucleons and pions, respectively. Solid dots refer to the lowest-order (dimension one) vertices from the chiral Lagrangian. Diagrams which result from the interchange of the nucleon lines and/or application of the time reversal operation are not shown.

details. In order to arrive at nuclear forces (and current operators) valid in the low-energy region (i.e., well below the pion production threshold), the pion fields need to be integrated out. This is achieved through decoupling of the purely nucleonic subspace of the Fock space from the rest via a suitably chosen unitary transformation (UT) [7–9]. This step is carried out perturbatively utilizing the chiral expansion and making use of the standard chiral power counting based on naive dimensional analysis. We also exploit the freedom to choose the basis states in the nucleonic subspace of the Fock space and include a large number of additional unitary transformations which can be constructed at the given chiral order [11]. It turns out that the resulting unitary ambiguity of the nuclear Hamiltonian and exchange currents is strongly constrained by requiring that the resulting nuclear potentials and currents are renormalizable; see [11] for a detailed discussion. The explicit form of the (purely strong) unitary transformation compatible with the renormalizability requirement and the operators contributing to effective nuclear Hamiltonian which are needed in the present calculation can be found in Appendix A (see also Ref. [11]). Once the unitary operator is determined at the desired order in the chiral expansion, the effective, purely nucleonic Hamiltonian can be computed straightforwardly. One ends up with terms given by a sequence of vertices and energy denominators which are similar to the ones emerging in time-ordered perturbation theory. However, the energy denominators and the coefficients in front of each term generally differ from the ones arising in the context of time-ordered perturbation theory. We refer to Ref. [15] for more details on the method of unitary transformation.

We now discuss the individual contributions to the three-nucleon force. Unless stated otherwise, the expressions for the 3N potentials are to be understood as matrix elements with respect to the nucleon momenta and as operators with respect to spin and isospin quantum numbers. We begin with diagrams (1)–(6) in Fig. 1 with one self-energy or vertex-correction insertion on the second nucleon. The contribution of these diagrams to the 3NF depends on the unitary transformations given in Eqs. (3.24), (3.25), and (3.48) of Ref. [11]. Fixing the corresponding rotation angles α_1, α_2, and α_6 in the way compatible with renormalizability as described in that work leads to the following result for the corresponding 3NF

contribution:

$$V = \frac{g_A^4 C_T}{4F_\pi^4}\boldsymbol{\tau}_1\cdot\boldsymbol{\tau}_2\frac{\vec{\sigma}_1\cdot\vec{q}_1}{q_1^2+M_\pi^2}\int\frac{d^3l}{(2\pi)^3}\frac{1}{\omega_l^4} \times[-(\vec{q}_1\cdot\vec{l})(\vec{l}\cdot\vec{\sigma}_3)+(\vec{q}_1\cdot\vec{\sigma}_3)\vec{l}^2] \overset{\text{DR}}{=} -\frac{g_A^4 C_T}{16\pi F_\pi^4}M_\pi\boldsymbol{\tau}_1\cdot\boldsymbol{\tau}_2\frac{(\vec{\sigma}_1\cdot\vec{q}_1)(\vec{\sigma}_3\cdot\vec{q}_1)}{q_1^2+M_\pi^2}, \quad (2.1)$$

where $\vec{\sigma}_i$ ($\boldsymbol{\tau}_i$) refer to the Pauli spin (isospin) matrices while $\vec{q}_i \equiv \vec{p}_i\,' - \vec{p}_i$ denote the momentum transfer of the nucleon i. Furthermore, g_A and F_π stay for the nucleon axial-vector and pion decay coupling constant, respectively, while C_T is the low-energy constant accompanying the lowest-order (spin-dependent) two-nucleon contact interaction. We emphasize that the Wigner-symmetry-invariant two-nucleon contact interaction proportional to C_S yields a vanishing contribution which can be traced back to the fact that it commutes with the pion-nucleon vertex. Here and in what follows, we use dimensional regularization (DR) in the derivation of the 3NF. Furthermore, we adopt the same notation as in Ref. [4] and give results for a particular choice of nucleon labels (unless stated otherwise). The full expression for the 3NF results by taking into account all possible permutations of the nucleons,[2] that is,

$$V_{3\text{N}}^{\text{full}} = V_{3\text{N}} + \text{all permutations}. \quad (2.2)$$

Next, the contribution of diagrams (7)–(9) in Fig. 1 with one self-energy or vertex-correction insertion on the third nucleon is found to vanish completely. This feature does not depend on the structure of vertices appearing in these diagrams and emerges from the renormalizability constraints; see Ref. [11]. On the other hand, diagrams (10)–(15) with pions being exchanged between the nucleons (1 and 2) and (2 and 3) do yield a nonvanishing contribution of the form

$$V = \frac{g_A^4 C_T}{4F_\pi^4}\frac{\vec{\sigma}_1\cdot\vec{q}_1}{q_1^2+M_\pi^2}\int\frac{d^3l}{(2\pi)^3}\frac{1}{\omega_l^4}\{\boldsymbol{\tau}_1\cdot\boldsymbol{\tau}_3[(\vec{q}_1\cdot\vec{l})(\vec{l}\cdot\vec{\sigma}_3)-(\vec{q}_1\cdot\vec{\sigma}_3)l^2]+(\boldsymbol{\tau}_1\times\boldsymbol{\tau}_2)\cdot\boldsymbol{\tau}_3\vec{l}\cdot(\vec{\sigma}_2\times\vec{\sigma}_3)\vec{q}_1\cdot\vec{l}\} \overset{\text{DR}}{=} \frac{g_A^4 C_T}{32\pi F_\pi^4}M_\pi\frac{\vec{\sigma}_1\cdot\vec{q}_1}{q_1^2+M_\pi^2}[2\boldsymbol{\tau}_1\cdot\boldsymbol{\tau}_3(\vec{q}_1\cdot\vec{\sigma}_3)-\boldsymbol{\tau}_1\cdot(\boldsymbol{\tau}_2\times\boldsymbol{\tau}_3)\vec{q}_1\cdot(\vec{\sigma}_2\times\vec{\sigma}_3)]. \quad (2.3)$$

We find that diagrams (16)–(18) involving a single self-energy or vertex-correction insertion on nucleon 1 do not generate 3NF contributions. For graph (17), this feature is quite general and does not depend on the vertex structure. Regardless of the choice for the additional unitary transformations, this diagram appears to be purely reducible at the order considered. Its contribution to the scattering amplitude is, therefore, properly accounted for by iterating the dynamical equation. The two self-energy corrections do yield nonvanishing irreducible contributions of opposite sign when considered separately. Since the leading nucleon self-energy correction is scalar, isoscalar, and independent of the nucleon momentum, the contributions of these two diagrams sum up to zero.

Similarly, diagrams (19)–(25) proportional to $g_A^2 C_{S,T}$ produce onlyvanishing 3NF contributions. This is because the integrands entering the corresponding loop integrals are always odd functions of the loop momentum. This feature depends crucially on the renormalizability constraints discussed above which ensure that the pion-exchange between the nucleons 1 and 2 factorizes out in all irreducible contributions emerging from these diagrams. Thus, the pion loop integrals are always proportional to ω_l^{-2} (which can be understood from the dimensional analysis) and involve a single power of the loop momentum $\vec{l}$ in the numerators emerging from the leading (derivative) pion-nucleon vertex ($\sim g_A$).

Next, diagrams (26) and (27) in Fig. 1, which are proportional to $g_A^2 C_S^2$ and $g_A^2 C_T^2$ also lead to vanishing 3NF contributions for the choices of the additional UTs compatible with the renormalizability constraints.[3] It should be emphasized that there are also purely short-range contributions to the 3NF $\propto g_A^2 C_S^2$ and $g_A^2 C_T$ emerging from diagrams shown in Fig. 2 with nucleon-nucleon (NN) contact interactions acting between different pairs of nucleons. While these graphs (presumably) generate nonvanishing 3NFs, their contributions are purely short-range and only provide a finite shift $\propto M_\pi$ to the LEC E which accompanies the contact 3NF at N^{2}LO. In any case, since we work with the bare LEC E, which needs to be refit to experimental data at each order in the chiral expansion, there is no need to explicitly evaluate these contributions unless one is interested in the quark mass dependence of the 3NF and few-nucleon observables.

Finally, the last two diagrams in Fig. 1 clearly do not yield any contributions in a complete analogy with next-to-leading-order (NLO) one-pion-exchange-contact diagrams. Finally,

[2]For three nucleons there are altogether 6 permutations.

[3]To avoid possible confusion, we emphasize once again that these diagrams correspond to all possible noniterative time-ordered graphs which nucleons treated as static sources. Nonstatic corrections are computed perturbatively, as discussed in Sec. IV.

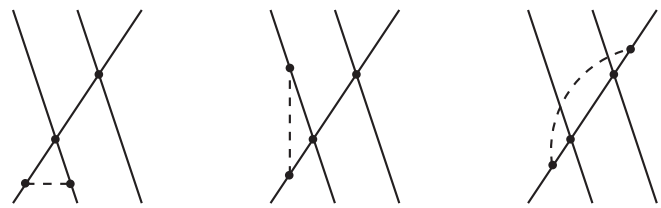

FIG. 2. Examples of diagrams $\propto g_A^2 C_{S,T}^2$ which lead to finite shifts of the purely short-range 3NF at N^{2}LO as explained in the text. For notation see Fig. 1.

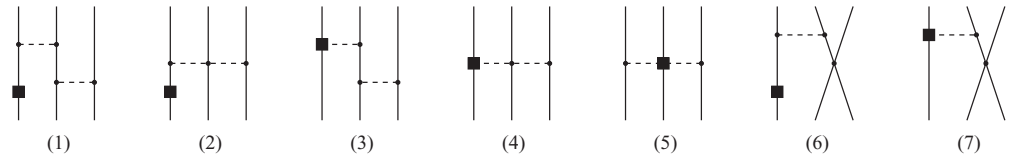

FIG. 3. Tree diagrams contributing to the two-pion-exchange and one-pion-exchange-contact topology of the 3NF at N^{3}LO. The solid boxes denote insertions of either subsubleading d_i vertices from the effective pion-nucleon Lagrangian or the leading $1/m$ corrections. For notation see Fig. 1.

there are also no contributions at N^{3}LO from tree diagrams involving one insertion of the higher-order d_i vertices in the effective Lagrangian [see graphs (6) and (7) in Fig. 3] except for the relativistic corrections which will be considered in Sec. IV. As explained in Ref. [4], the contributions from these diagrams are suppressed by at least one power of Q/m where Q denotes a genuine soft scale.

We are thus left with Eqs. (2.1) and (2.3) as the only nonvanishing contributions to the one-pion-exchange-contact 3NF topology. We now show that these terms cancel each other exactly if one takes into account the antisymmetric nature of few-nucleon states. In particular, we use the identities

$$\begin{aligned}\left(\boldsymbol{\tau}_3\sigma_3^i+\boldsymbol{\tau}_2\sigma_2^i\right)_{\mathrm{A23}} &= \tfrac{1}{4}\big(\boldsymbol{\tau}_3\sigma_3^i+\boldsymbol{\tau}_2\sigma_2^i-\boldsymbol{\tau}_3\sigma_2^i-\boldsymbol{\tau}_2\sigma_3^i\\ &\quad+\boldsymbol{\tau}_2\times\boldsymbol{\tau}_3[\vec{\sigma}_2\times\vec{\sigma}_3]^i\big)\equiv\boldsymbol{B}^i,\\ (\boldsymbol{\tau}_2\times\boldsymbol{\tau}_3[\vec{\sigma}_2\times\vec{\sigma}_3]^i)_{\mathrm{A23}} &= 2\boldsymbol{B}^i,\\ \left(\boldsymbol{\tau}_3\sigma_2^i+\boldsymbol{\tau}_2\sigma_3^i\right)_{\mathrm{A23}} &= -\boldsymbol{B}^i,\end{aligned}\tag{2.4}$$

where the superscript i refers to the Cartesian component of the Pauli spin matrices and A23 denotes antisymmetrization with respect to nucleons 2 and 3, which, for a momentum-independent operator X, can be written in the form

$$(X)_{\mathrm{A23}}\equiv\frac{1}{2}\left(X-\frac{1+\vec{\sigma}_2\cdot\vec{\sigma}_3}{2}\frac{1+\boldsymbol{\tau}_2\cdot\boldsymbol{\tau}_3}{2}X\right).\tag{2.5}$$

It is easy to see that adding the contribution from interchanging the nucleons 2 and 3 to Eqs. (2.1) and (2.3) and performing antisymmetrization with respect to these nucleons leads to a vanishing result. Therefore, we conclude that there are no one-pion-exchange-contact terms in the 3NF at N^{3}LO.

III. TWO-PION-EXCHANGE-CONTACT TOPOLOGY

We now turn to the two-pion-exchange-contact diagrams shown in Fig. 4. Evaluating the matrix elements of the operators listed in Eq. (A1)

for diagrams (1)–(7) in this figure we find the $g_A^4C_S$ and $g_A^4C_T$ contributions to the two-pion-exchange-contact topology of the form

$$\begin{aligned}V_{2\pi\text{-cont}} &= \frac{g_A^4C_T}{8F_\pi^4}\int\frac{d^3l}{(2\pi)^3}\Bigg[\boldsymbol{\tau}_1\cdot\boldsymbol{\tau}_2\Bigg\{\left(\frac{1}{\omega_+^4\omega_-^2}+\frac{1}{\omega_+^2\omega_-^4}\right)\big[q_1^2\,(\vec{q}_1\cdot\vec{\sigma}_2)\,(\vec{q}_1\cdot\vec{\sigma}_3)\;+2q_1^2l^2\,(\vec{\sigma}_2\cdot\vec{\sigma}_3)-q_1^2(\vec{l}\cdot\vec{\sigma}_2)(\vec{l}\cdot\vec{\sigma}_3)\\ &\quad-q_1^4\,(\vec{\sigma}_2\cdot\vec{\sigma}_3)-l^2(\vec{q}_1\cdot\vec{\sigma}_2)(\vec{q}_1\cdot\vec{\sigma}_3)+l^2(\vec{l}\cdot\vec{\sigma}_2)(\vec{l}\cdot\vec{\sigma}_3)-l^4(\vec{\sigma}_2\cdot\vec{\sigma}_3)\big]+\left(\frac{1}{\omega_+^4\omega_-^2}-\frac{1}{\omega_+^2\omega_-^4}\right)\\ &\quad\times\big[-q_1^2(\vec{q}_1\cdot\vec{\sigma}_2)(\vec{l}\cdot\vec{\sigma}_3)+q_1^2(\vec{l}\cdot\vec{\sigma}_2)(\vec{q}_1\cdot\vec{\sigma}_3)+l^2(\vec{q}_1\cdot\vec{\sigma}_2)(\vec{l}\cdot\vec{\sigma}_3)-l^2(\vec{l}\cdot\vec{\sigma}_2)(\vec{q}_1\cdot\vec{\sigma}_3)\big]\Bigg\}\\ &\quad+2\boldsymbol{\tau}_2\cdot\boldsymbol{\tau}_3\left(\frac{1}{\omega_+^4\omega_-^2}+\frac{1}{\omega_+^2\omega_-^4}\right)\big[q_1^2l^2(\vec{\sigma}_1\cdot\vec{\sigma}_2)+q_1^2(\vec{l}\cdot\vec{\sigma}_1)(\vec{l}\cdot\vec{\sigma}_2)+(\vec{q}_1\cdot\vec{l})(\vec{q}_1\cdot\vec{\sigma}_1)(\vec{l}\cdot\vec{\sigma}_2)\\ &\quad+(\vec{q}_1\cdot\vec{l})(\vec{l}\cdot\vec{\sigma}_1)(\vec{q}_1\cdot\vec{\sigma}_2)-(\vec{q}_1\cdot\vec{l})^2(\vec{\sigma}_1\cdot\vec{\sigma}_2)-l^2(\vec{q}_1\cdot\vec{\sigma}_1)(\vec{q}_1\cdot\vec{\sigma}_2)\big]+6\left(\frac{1}{\omega_+^4\omega_-^2}+\frac{1}{\omega_+^2\omega_-^4}\right)\\ &\quad\times\big[-q_1^2l^2(\vec{\sigma}_1\cdot\vec{\sigma}_2)+q_1^2(\vec{l}\cdot\vec{\sigma}_1)(\vec{l}\cdot\vec{\sigma}_2)-(\vec{q}_1\cdot\vec{l})(\vec{q}_1\cdot\vec{\sigma}_1)(\vec{l}\cdot\vec{\sigma}_2)\\ &\quad-(\vec{q}_1\cdot\vec{l})(\vec{l}\cdot\vec{\sigma}_1)(\vec{q}_1\cdot\vec{\sigma}_2)+(\vec{q}_1\cdot\vec{l})^2(\vec{\sigma}_1\cdot\vec{\sigma}_2)+l^2(\vec{q}_1\cdot\vec{\sigma}_1)(\vec{q}_1\cdot\vec{\sigma}_2)\big]\Bigg]\\ &\overset{\mathrm{DR}}{=}\frac{g_A^4C_T}{48\pi F_\pi^4}\Bigg\{2\boldsymbol{\tau}_1\cdot\boldsymbol{\tau}_2(\vec{\sigma}_2\cdot\vec{\sigma}_3)\left[3M_\pi-\frac{M_\pi^3}{4M_\pi^2+q_1^2}+2\big(2M_\pi^2+q_1^2\big)A(q_1)\right]\\ &\quad+9\left[(\vec{q}_1\cdot\vec{\sigma}_1)(\vec{q}_1\cdot\vec{\sigma}_2)-q_1^2(\vec{\sigma}_1\cdot\vec{\sigma}_2)\right]A(q_1)\Bigg\},\end{aligned}\tag{3.1}$$

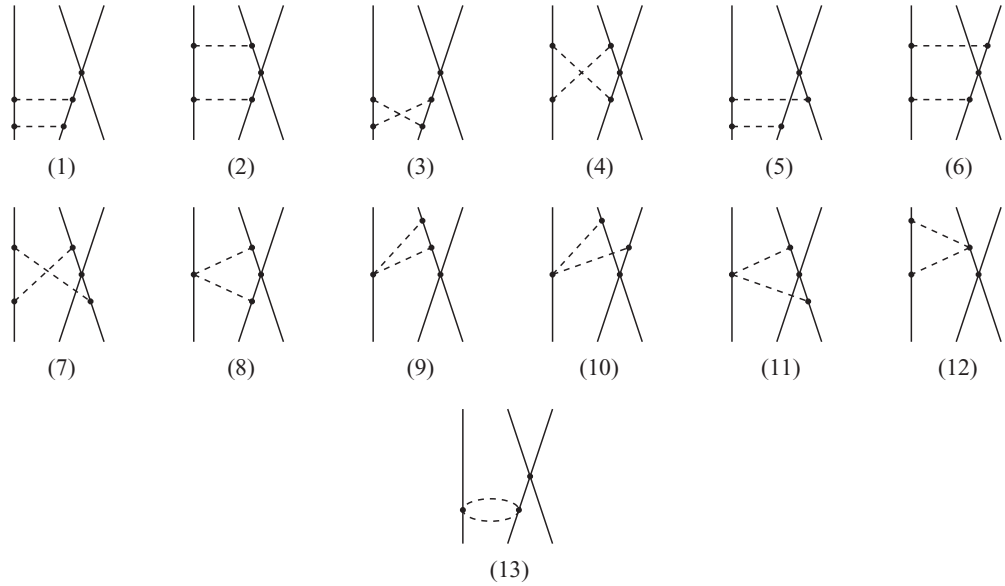

FIG. 4. Diagrams contributing to the two-pion-exchange-contact topology of the 3NF. For notation see Fig. 1.

where the loop function $A(q)$ is defined according to

$$A(q) = \frac{1}{2q} \arctan\left(\frac{q}{2M_\pi}\right). \tag{3.2}$$

Notice that we have exploited the fermionic nature of the nucleons in order to simplify the above expression and made use of the following identities:

$$\begin{aligned}\left[(\boldsymbol{\tau}_2+\boldsymbol{\tau}_3)\sigma_2^i\sigma_3^j\right]_{\mathrm{A23}} &= -\tfrac{1}{4}(\boldsymbol{\tau}_2+\boldsymbol{\tau}_3)\delta_{ij}(1-\vec{\sigma}_2\cdot\vec{\sigma}_3)+\cdots,\\ \left[\boldsymbol{\tau}_2\cdot\boldsymbol{\tau}_3(\vec{\sigma}_2+\vec{\sigma}_3)\right]_{\mathrm{A23}} &= -3\,(\vec{\sigma}_2+\vec{\sigma}_3)_{\mathrm{A23}}\\ &= -\tfrac{3}{4}(\vec{\sigma}_2+\vec{\sigma}_3)+\tfrac{3}{4}\boldsymbol{\tau}_2\cdot\boldsymbol{\tau}_3(\vec{\sigma}_2+\vec{\sigma}_3),\end{aligned} \tag{3.3}$$

where the ellipses in the first line refer to terms which are antisymmetric with respect to the interchange of the indices i, j and therefore do not contribute to the final result.

We now turn to diagrams (8)–(12) in Fig. 4 whose contributions are proportional to $g_A^2 C_{S,T}$. We find that graph (12) does not contain any irreducible pieces, while the contributions of diagrams (8)–(11) reads

$$\begin{aligned}V_{2\pi\text{-cont}} = \frac{g_A^2}{32F_\pi^4}\int\frac{d^3l}{(2\pi)^3}\frac{1}{\omega_+^2\omega_-^2}\big[&i(C_S+C_T)[\boldsymbol{\tau}_1\times\boldsymbol{\tau}_2]\cdot\boldsymbol{\tau}_3\\ &\times[-(\vec{q}_1\cdot\vec{\sigma}_2)(\vec{l}\cdot\vec{\sigma}_3)+(\vec{l}\cdot\vec{\sigma}_2)(\vec{q}_1\cdot\vec{\sigma}_3)]\\ &+4C_T\boldsymbol{\tau}_1\cdot\boldsymbol{\tau}_2\big\{-q_1^2(\vec{\sigma}_2\cdot\vec{\sigma}_3)+(\vec{q}_1\cdot\vec{\sigma}_2)(\vec{q}_1\cdot\vec{\sigma}_3)\\ &+l^2(\vec{\sigma}_2\cdot\vec{\sigma}_3)-(\vec{l}\cdot\vec{\sigma}_2)(\vec{l}\cdot\vec{\sigma}_3)-2i[\vec{q}_1\times\vec{l}]\cdot\vec{\sigma}_3\big\}\big].\end{aligned} \tag{3.4}$$

It is easy to see that all terms involving the imaginary unit number i are vanishing. Using dimensional regularization and performing antisymmetrization with respect to the nucleons 2 and 3 we arrive at the following final result for the $g_A^2 C_S$ and $g_A^2 C_T$ contributions to $V_{2\pi\text{-cont}}$:

$$V_{2\pi\text{-cont}} \overset{\mathrm{DR}}{=} -\frac{g_A^2 C_T}{24\pi F_\pi^4}\boldsymbol{\tau}_1\cdot\boldsymbol{\tau}_2(\vec{\sigma}_2\cdot\vec{\sigma}_3)\big[M_\pi+\big(2M_\pi^2+q_1^2\big)A(q_1)\big]. \tag{3.5}$$

Finally, it is easy to see that the last diagram in Fig. 4 does not contribute to 3NF as the corresponding Feynman graph involves at this order in the chiral expansion only reducible pieces. To summarize, the complete contribution of the two-pion-exchange-contact topology of the 3NF at N^{3}LO is given by Eqs. (3.1) and (3.5) using the convention of Eq. (2.2).

IV. LEADING RELATIVISTIC CORRECTIONS

The leading relativistic corrections (i.e., the corrections of the operators in $1/m$) to the 3NF provide further contributions to the two-pion-exchange and one-pion-exchange-contact topologies. They emerge from two different sources. We remind the reader that the formally leading 3NF generated by the tree-level two-pion-exchange[4] and one-pion-exchange contact diagrams vanishes at NLO. Stated differently, the resulting contributions to the scattering amplitude are either purely reducible (at that order) or shifted to N^{3}LO due to the suppression by one power of Q/m caused by the time derivative entering the Weinberg-Tomozawa vertex [16,17]. The first kind of relativistic correction emerges from taking into account retardation effects in NLO diagrams; see graphs (1), (2), and (6) in Fig. 3. As will be shown below and contrary to the case when the nucleons are treated as static sources, these diagrams do produce nonvanishing 3NFs. Second, one also needs to take into account the $1/m$ corrections to the leading

[4]There are two such diagrams: one proportional to g_A^4 and one involving a Weinberg-Tomozawa vertex, which is proportional to g_A^2.

πNN and $\pi\pi NN$ vertices which leads to graphs (3), (4), (5), and (7) in Fig. 3. Notice that there are no $1/m$ corrections to the leading two-nucleon contact interactions.

We begin with the retardation corrections to the two-pion exchange 3NF corresponding to diagram (1) in Fig. 3. When evaluating its contribution to the potential, one needs, in addition to the terms listed in Eq. (A.1) of Ref. [11], to take into account effects induced by the additional unitary transformation driven by the operator S_8 in Eq. (4.14) of Ref. [13], which is parametrized in that work by a constant $\bar{\beta}_8$. The explicit form of the operators to be evaluated is given in Eq. (A3). The resulting 3NF contribution has the form

$$\begin{aligned} V_{2\pi,1/m} = &-\frac{g_A^4}{32mF_\pi^4}\frac{(\vec{\sigma}_1\cdot\vec{q}_1)(\vec{\sigma}_3\cdot\vec{q}_3)}{\left(q_1^2+M_\pi^2\right)^2\left(q_3^2+M_\pi^2\right)}[(1-2\bar{\beta}_8)\{\boldsymbol{\tau}_1\cdot\boldsymbol{\tau}_3 \\ &\times(\vec{q}_1\cdot\vec{q}_3)^2+[\boldsymbol{\tau}_1\times\boldsymbol{\tau}_2]\cdot\boldsymbol{\tau}_3[\vec{q}_1\times\vec{q}_3]\cdot\vec{\sigma}_2(\vec{q}_1\cdot\vec{q}_3)\} \\ &-2i\{\boldsymbol{\tau}_1\cdot\boldsymbol{\tau}_3[\vec{q}_1\times\vec{q}_3]\cdot\vec{\sigma}_2-[\boldsymbol{\tau}_1\times\boldsymbol{\tau}_2]\cdot\boldsymbol{\tau}_3(\vec{q}_1\cdot\vec{q}_3)\} \\ &\times\{(1-2\bar{\beta}_8)(\vec{q}_1\cdot\vec{k}_2)+(1+2\bar{\beta}_8)(\vec{q}_1\cdot\vec{k}_1)\}], \end{aligned} \tag{4.1}$$

where $\vec{k}_i\equiv(\vec{p}_i+\vec{p}_i\,')/2$. Notice that the unitary transformation considered above also affects the form of the $1/m^2$ corrections to the one-pion exchange and $1/m$ corrections to the two-pion exchange two-nucleon potentials at N^{3}LO. To be consistent with the N^{3}LO potential of Ref. [10], one has to choose $\bar{\beta}_8=1/4$. The contribution of diagram (2) in Fig. 3 is not affected by the above UT and has the form

$$\begin{aligned} V_{2\pi,1/m} = &\, i\frac{g_A^2}{32mF_\pi^4}\frac{(\vec{\sigma}_1\cdot\vec{q}_1)(\vec{\sigma}_3\cdot\vec{q}_3)}{\left(q_1^2+M_\pi^2\right)\left(q_3^2+M_\pi^2\right)} \\ &\times[\boldsymbol{\tau}_1\times\boldsymbol{\tau}_2]\cdot\boldsymbol{\tau}_3(\vec{q}_3\cdot\vec{k}_3-\vec{q}_1\cdot\vec{k}_1). \end{aligned} \tag{4.2}$$

Finally, retardation corrections to the one-pion-exchange-contact topology from diagram (6) in Fig. 3 have the form

$$\begin{aligned} V_{1\pi\text{-cont},1/m} = &\frac{g_A^2}{8mF_\pi^2}\frac{\vec{\sigma}_1\cdot\vec{q}_1}{\left(q_1^2+M_\pi^2\right)^2}\boldsymbol{\tau}_1\cdot\boldsymbol{\tau}_2 \\ &\times\{(1-2\bar{\beta}_8)(\vec{q}_1\cdot\vec{q}_3)[C_S(\vec{q}_1\cdot\vec{\sigma}_2)+C_T(\vec{q}_1\cdot\vec{\sigma}_3)] \\ &+2iC_T\vec{q}_1\cdot[\vec{\sigma}_2\times\vec{\sigma}_3][(1-2\bar{\beta}_8)(\vec{q}_1\cdot\vec{k}_2) \\ &+(1+2\bar{\beta}_8)(\vec{q}_1\cdot\vec{k}_1)]\}. \end{aligned} \tag{4.3}$$

We now turn to contributions emerging from relativistic corrections to vertices in the pion-nucleon Hamilton density. Consider first the contributions of diagrams (3), (4), and (7) in Fig. 3. The relevant terms in the effective Lagrangian and Hamiltonian have the form[5]

$$\begin{aligned} \mathcal{L}_{\pi N} = -\mathcal{H}_{\pi N} = &-\frac{g_A}{2F_\pi}N^\dagger\boldsymbol{\tau}\vec{\sigma}\cdot\vec{\nabla}\boldsymbol{\pi}N \\ &-i\frac{g_A}{4mF_\pi}N^\dagger\boldsymbol{\tau}\vec{\sigma}\cdot(\overleftarrow{\nabla}-\overrightarrow{\nabla})N\cdot\dot{\boldsymbol{\pi}}, \end{aligned} \tag{4.4}$$

where N and $\boldsymbol{\pi}$ refer to the nucleon and pion fields, respectively. Similarly to the retardation corrections considered above, it is possible to construct an additional UT with the generator proportional to g_A^2/m which affects the contributions of diagrams (3) and (7) when acting on the one-pion exchange and the leading contact potentials, respectively. We adopt here the notation of Ref. [13], where this unitary operator is parameterized in terms of another arbitrary parameter $\bar{\beta}_9$, see Eq. (4.14) of that work. Again, the UT also affects the $1/m^2$ and $1/m$ corrections to the one-pion and two-pion exchange potential at N^{3}LO, respectively, so that the parameter $\bar{\beta}_9$ needs to be chosen consistently. Using the explicit expressions for the operator structure of the unitarily transformed Hamilton operator in Eq. (A.4) of Ref. [11] and adding terms induced by the above mentioned UT we obtain the following 3NF contribution from diagram (3):

$$\begin{aligned} V_{2\pi,1/m} = &-\frac{g_A^4}{32mF_\pi^4}\frac{\vec{\sigma}_1\cdot\vec{q}_1}{\left(q_1^2+M_\pi^2\right)\left(q_3^2+M_\pi^2\right)}\{\boldsymbol{\tau}_1\cdot\boldsymbol{\tau}_3 \\ &\times[(2\bar{\beta}_9-1)(\vec{\sigma}_3\cdot\vec{q}_3)(q_1^2+2i[\vec{q}_1\times\vec{k}_2]\cdot\vec{\sigma}_2) \\ &-2i(2\bar{\beta}_9+1)(\vec{\sigma}_3\cdot\vec{k}_3)[\vec{q}_1\times\vec{q}_3]\cdot\vec{\sigma}_2] \\ &+2i[\boldsymbol{\tau}_1\times\boldsymbol{\tau}_2]\cdot\boldsymbol{\tau}_3[-(2\bar{\beta}_9-1)(\vec{\sigma}_3\cdot\vec{q}_3)(\vec{q}_1\cdot\vec{k}_2) \\ &+(2\bar{\beta}_9+1)(\vec{\sigma}_3\cdot\vec{k}_3)(\vec{q}_1\cdot\vec{q}_3)]\}. \end{aligned} \tag{4.5}$$

Next, it is easy to see that diagram (4) does not generate any 3NF at the considered order in the chiral expansion. Similarly to the corresponding NLO diagram (same topology constructed from the lowest-order vertices), there is suppression by, in this case, two factors of Q/m due to the time derivatives entering the Weinberg-Tomozawa vertex and the $1/m$ correction to the πNN vertex in Eq. (4.4). Consequently, within the power-counting scheme adopted in the present work, this diagram contributes to the 3NF only at order N^{5}LO. Finally, the contribution of diagram (7) in Fig. 3 is clearly also affected by the above-mentioned unitary transformation and is given by

$$\begin{aligned} V_{1\pi\text{-cont},1/m} = &-\frac{g_A^2C_T}{8mF_\pi^2}\frac{1}{q_1^2+M_\pi^2}\boldsymbol{\tau}_1\cdot\boldsymbol{\tau}_2\{2i(2\bar{\beta}_9+1)(\vec{k}_1\cdot\vec{\sigma}_1) \\ &\times\vec{q}_1\cdot[\vec{\sigma}_2\times\vec{\sigma}_3]-\left(2\bar{\beta}_9-1\right)(\vec{q}_1\cdot\vec{\sigma}_1)(\vec{q}_3\cdot\vec{\sigma}_3) \\ &-2i(2\bar{\beta}_9-1)(\vec{q}_1\cdot\vec{\sigma}_1)\vec{k}_2\cdot[\vec{\sigma}_2\times\vec{\sigma}_3]\} \\ &+\frac{g_A^2C_S}{8mF_\pi^2}\frac{1}{q_1^2+M_\pi^2}\boldsymbol{\tau}_1\cdot\boldsymbol{\tau}_2 \\ &\times(2\bar{\beta}_9-1)(\vec{q}_1\cdot\vec{\sigma}_1)(\vec{q}_3\cdot\vec{\sigma}_2). \end{aligned} \tag{4.6}$$

Finally, consider the contribution of diagram (5). Since this graph does not induce any reducible pieces, the corresponding 3NF can be identified with the amplitude and computed using the Feynman-diagram technique. The Feynman rule for the $1/m$ correction to the $\pi\pi NN$ vertex can be found, for example, Ref. [19]. In our notation the relevant terms[6] have

[5]Different conventions for the sign of the axial vector coupling constant g_A are used in the literature. For example, g_A in Ref. [18] corresponds to $-g_A$ in the present work. This difference does not affect the expressions for nuclear forces and currents where the LEC g_A enters quadratically. It is important, however, to use the same convention for both terms in Eq. (4.4).

[6]We do not show terms involving zeroth components of the nucleon momenta since they do not contribute to the 3NF at N^{3}LO.

the form

$$-\frac{1}{8mF_\pi^2}\epsilon^{abc}\tau^c(\vec{p}+\vec{p}\,')\cdot(\vec{q}_1+\vec{q}_2)$$
$$-\frac{i}{4mF_\pi^2}\epsilon^{abc}\tau^c[\vec{q}_1\times\vec{q}_2]\cdot\vec{\sigma}, \qquad (4.7)$$

where $\vec{q}_1, a$ ($\vec{q}_2, b$) denote the momentum and isospin quantum number of the incoming (outgoing) pion. We then obtain for the contribution of diagram (5)

$$V_{2\pi,1/m}=\frac{g_A^2}{32mF_\pi^4}\frac{(\vec{\sigma}_1\cdot\vec{q}_1)(\vec{\sigma}_3\cdot\vec{q}_3)}{\left(q_1^2+M_\pi^2\right)\left(q_3^2+M_\pi^2\right)}[\boldsymbol{\tau}_1\times\boldsymbol{\tau}_3]\cdot\boldsymbol{\tau}_2$$
$$\times([\vec{q}_1\times\vec{q}_3]\cdot\vec{\sigma}_2+i\vec{k}_2\cdot(\vec{q}_3-\vec{q}_1)). \qquad (4.8)$$

To summarize, our results for the relativistic $(1/m)$ corrections to the 3NF at N^{3}LO are given by Eqs. (4.1)–(4.3), (4.5), (4.6), and (4.8). Adding up these expressions, the two-pion exchange contribution can be written in the form

$$V_{2\pi,1/m}=\frac{g_A^2}{32mF_\pi^4}\frac{1}{\left(q_1^2+M_\pi^2\right)\left(q_3^2+M_\pi^2\right)}(\boldsymbol{\tau}_1\cdot\boldsymbol{\tau}_3A_{123}$$
$$+[\boldsymbol{\tau}_1\times\boldsymbol{\tau}_2]\cdot\boldsymbol{\tau}_3B_{123})+5\text{ permutations}, \qquad (4.9)$$

where

$$A_{123}=(\vec{\sigma}_1\cdot\vec{q}_1)(\vec{\sigma}_3\cdot\vec{q}_3)a_{123}+(\vec{\sigma}_1\cdot\vec{q}_1)(\vec{\sigma}_3\cdot\vec{k}_3)c_{123},$$
$$B_{123}=(\vec{\sigma}_1\cdot\vec{q}_1)(\vec{\sigma}_3\cdot\vec{q}_3)b_{123}+(\vec{\sigma}_1\cdot\vec{q}_1)(\vec{\sigma}_3\cdot\vec{k}_3)d_{123}, \qquad (4.10)$$

and the functions a_{123}, b_{123}, c_{123}, and d_{123} are given by

$$a_{123}=-\frac{g_A^2}{q_1^2+M_\pi^2}\{(1-2\bar{\beta}_8)(\vec{q}_1\cdot\vec{q}_3)^2-2i[\vec{q}_1\times\vec{q}_3]\cdot\vec{\sigma}_2$$
$$\times[(1-2\bar{\beta}_8)(\vec{q}_1\cdot\vec{k}_2)+(1+2\bar{\beta}_8)(\vec{q}_1\cdot\vec{k}_1)]\}$$
$$-g_A^2(2\bar{\beta}_9-1)\left(q_1^2+2i[\vec{q}_1\times\vec{k}_2]\cdot\vec{\sigma}_2\right),$$
$$c_{123}=2ig_A^2\left(2\bar{\beta}_9+1\right)[\vec{q}_1\times\vec{q}_3]\cdot\vec{\sigma}_2,$$
$$b_{123}=-\frac{g_A^2}{q_1^2+M_\pi^2}\{(1-2\bar{\beta}_8)[\vec{q}_1\times\vec{q}_3]\cdot\vec{\sigma}_2(\vec{q}_1\cdot\vec{q}_3)+2i(\vec{q}_1\cdot\vec{q}_3)$$
$$\times[(1-2\bar{\beta}_8)(\vec{q}_1\cdot\vec{k}_2)+(1+2\bar{\beta}_8)(\vec{q}_1\cdot\vec{k}_1)]\}$$
$$+2i\vec{q}_3\cdot(\vec{k}_3-\vec{k}_2)+2ig_A^2(2\bar{\beta}_9-1)(\vec{q}_1\cdot\vec{k}_2)$$
$$-[\vec{q}_1\times\vec{q}_3]\cdot\vec{\sigma}_2,$$
$$d_{123}=-2ig_A^2(2\bar{\beta}_9+1)(\vec{q}_1\cdot\vec{q}_3). \qquad (4.11)$$

The relativistic corrections to the one-pion-exchange-contact topology have the form

$$V_{1\pi\text{-cont},1/m}=\frac{g_A^2}{8mF_\pi^2}\frac{1}{q_1^2+M_\pi^2}\boldsymbol{\tau}_1\cdot\boldsymbol{\tau}_2$$
$$\times[(\vec{\sigma}_1\cdot\vec{q}_1)f_{123}+(\vec{\sigma}_1\cdot\vec{k}_1)g_{123}]+5\text{ permutations}, \qquad (4.12)$$

where

$$f_{123}=\frac{1}{q_1^2+M_\pi^2}\{(1-2\bar{\beta}_8)(\vec{q}_1\cdot\vec{q}_3)[C_S(\vec{q}_1\cdot\vec{\sigma}_2)$$
$$+C_T(\vec{q}_1\cdot\vec{\sigma}_3)]+2iC_T\vec{q}_1\cdot[\vec{\sigma}_2\times\vec{\sigma}_3][(1-2\bar{\beta}_8)(\vec{q}_1\cdot\vec{k}_2)$$
$$+(1+2\bar{\beta}_8)(\vec{q}_1\cdot\vec{k}_1)]\}+(2\bar{\beta}_9-1)[C_S(\vec{q}_3\cdot\vec{\sigma}_2)$$
$$+C_T(\vec{q}_3\cdot\vec{\sigma}_3)]+2iC_T(2\bar{\beta}_9-1)\vec{k}_2\cdot[\vec{\sigma}_2\times\vec{\sigma}_3],$$
$$g_{123}=-2iC_T(2\bar{\beta}_9+1)\vec{q}_1\cdot[\vec{\sigma}_2\times\vec{\sigma}_3]. \qquad (4.13)$$

The above expressions are written in a general form including the dependence on the constants $\bar{\beta}_8$ and $\bar{\beta}_9$ which parametrize the unitary ambiguity of these potentials. The $1/m^2$ corrections ($1/m$ corrections) to the one-pion exchange (two-pion-exchange) two-nucleon potential at N^{3}LO are also affected by this unitary ambiguity. A comprehensive discussion on this issue and on the relation between different forms of relativistic extensions of the Schrödinger equation and nonstatic terms in the two-nucleon potential can be found in Ref. [20]. To be consistent with the two-nucleon potential of Ref. [10], one needs to choose

$$\bar{\beta}_8=\frac{1}{4},\quad \bar{\beta}_9=0. \qquad (4.14)$$

We emphasize that, in order to completely take into account the relativistic corrections at N^{3}LO in few-body calculations, one needs to use the Schrödinger equation with the relativistic expression for the nucleon kinetic energy, the proper forms of the $1/m^2$ corrections to the 1π-exchange NN potential, as well as $1/m$ corrections to the NN and 3N forces. In addition, one has to take into account boost corrections to the leading-order two-nucleon potential (i.e., the $\vec{P}$ dependence in the 1π-exchange potential and the leading contact interactions; see Ref. [21]).

While $1/m$ corrections to the one-pion-exchange-contact 3NF given in Eq. (4.12) have been never considered before, the leading relativistic corrections to the two-pion exchange 3NF were studied by Friar and Coon in Ref. [22]; however, they only provide expressions in coordinate space. In order to facilitate a comparison between our results and the ones by Friar and Coon, we give in Appendix B the coordinate-space representation of the obtained 3NF contributions. Our profile functions are related to the one used in Ref. [22] according to

$$U_1(M_\pi r)=\frac{4\pi}{M_\pi}h_0(r),\quad \vec{\nabla}_{\vec{r}}U_2(M_\pi r)=-4\pi M_\pi\vec{r}\,h_0(r), \qquad (4.15)$$

where the function h_0 is defined in Eq. (24c) of that work. Furthermore, $f^2\,(M)$ in Ref. [22] correspond to $[g_A/(2F_\pi)]^2\,(m)$ in our notation. Friar and Coon also discuss the unitary ambiguity of the resulting 3N potentials associated with the UTs $\propto 1/m$. They parametrized it in terms of the arbitrary parameters μ and ν; see also Ref. [20]. The relations between their μ, ν and our $\bar{\beta}_8$ and $\bar{\beta}_9$ are given by

$$\mu=4\bar{\beta}_9+1,\quad \nu=2\bar{\beta}_8. \qquad (4.16)$$

Taking into account the typographical error in [22] as pointed out in [5] of Ref. [20], we observe that our results for the $1/m$ corrections to the two-pion exchange 3NF in Eqs.(B3)–(B5) agree with the ones in Eqs. (23a)– (23c) and (33a)–(33d) of

Ref. [22] except for the retardation corrections in $\tilde{a}_{123}$ and $\tilde{b}_{123}$ emerging from diagram (1) in Fig. 3. More precisely, we reproduce the results of Friar and Coon if we make the replacement

$$(1-2\bar{\beta}_8)(\vec{q}_1\cdot\vec{k}_2)+(1+2\bar{\beta}_8)(\vec{q}_1\cdot\vec{k}_1)\to (1-2\bar{\beta}_8)(\vec{q}_1\cdot\vec{k}_2)+(1+2\bar{\beta}_8)(\vec{q}_1\cdot\vec{k}_1)+\delta \quad (4.17)$$

in a_{123} and b_{123} in Eq. (4.11) with δ given by

$$\delta=(1-2\bar{\beta}_8)\vec{q}_1\cdot(\vec{k}_2-\vec{k}_1)+(1-2\bar{\beta}_8)\vec{q}_3\cdot(\vec{k}_2-\vec{k}_3) =\tfrac{1}{2}\big(1-2\bar{\beta}_8\big)\big(p_1^2+p_2^2+p_3^2-p_1'^{\,2}-p_2'^{\,2}-p_3'^{\,2}\big), \quad (4.18)$$

where we made use of the identity $\vec{q}_1+\vec{q}_2+\vec{q}_3=0$. This implies that the difference between our results appears only when the nucleons are off-the-energy shell. We conjecture that this difference originates from the additional UTs $\exp(\alpha_1 S_1+\alpha_2 S_2)$ with α_1 and α_2 denoting the transformation angles and S_1 and S_2 denoting the generators of the two-pion-exchange range whose explicit form is given in Eq. (3.25) of Ref. [11]. The corresponding unitary ambiguity is not explored by Friar and Coon. It is easy to see that these UTs induce, among others, terms in the 3NF $\propto [E_{\rm kin},(\alpha_1 S_1+\alpha_2 S_2)]$ which have the same structure as the δ terms discussed above. As explained in Ref. [11], the angles α_1 and α_2 have to be chosen in a specific way [see Eq. (3.31) of that work] in order to maintain renormalizability of the leading loop corrections to the 3NF. Our findings therefore indicate that the particular choice made in Ref. [22] for α_1 and α_2 is not compatible with the above-mentioned renormalizability constraint.

V. SUMMARY AND CONCLUSIONS

In this work, we have derived the short-range part and the relativistic $(1/m)$ corrections to the 3NF in chiral effective field theory at N^{3}LO. Combined with the long-range parts already given in Ref. [4], this completes the calculation of two-, three-, and four-nucleon forces at this order in the formulation without explicit $\Delta(1232)$ degrees of freedom. The short-range parts considered here consists formally of two different topologies. Remarkably, there is no contribution from the one-pion-exchange-contact topology at N^{3}LO as we have demonstrated in Sec. II. The total contribution from the two-pion-exchange-contact topology is given in Eqs. (3.1) and (3.5) supplemented with Eq. (2.2). Furthermore, there are relativistic $(1/m)$ corrections to the leading 3NF at N^{2}LO, which are worked out in Sec. IV. The corresponding terms of the 3NF are summarized in Eqs. (4.9) and (4.12). We also provide the coordinate-space representation of the obtained results in Appendix B and compare our findings for the long-range $1/m$ corrections with the earlier calculation by Friar and Coon [22].

We stress again that at N^{3}LO, the 3NF is free of unknown LECs, so the complete 3NF consisting of terms at N^{2}LO and N^{3}LO contains altogether only the two LECs D and E which need to be determined from few-nucleon data. With the results presented here, one is now in the position to analyze in detail the many data in few-nucleon and heavier systems based on consistent and precise two- and three-nucleon forces. In particular, it will be interesting to find out whether the remaining discrepancies in the three- and four-nucleon systems will be overcome employing the force derived in Ref. [4] and here. Work along these lines is in progress.

ACKNOWLEDGMENTS

This work was supported by funds provided by the Helmholtz Association (Grants No. VH-NG-222 and No. VH-VI-231), by the DFG (SFB/TR 16 "Subnuclear Structure of Matter"), by the EU HadronPhysics2 project "Study of strongly interacting matter" and the European Research Council (ERC-2010-StG 259218 NuclearEFT), and by BMBF (Grant No. 06BN9006).

APPENDIX A: FORMAL ALGEBRAIC STRUCTURE OF THE 3NF CORRECTIONS

In this appendix we list the formal operator structure of the various N^{3}LO contributions to the nuclear Hamiltonian relevant for the present calculations. A detailed discussion on these terms can be found in Ref. [11]. We include contributions induced by the additional UTs considered in that work and in Eq. (4.23) of Ref. [13]. Except for α_5, $\bar{\beta}_8$, and $\bar{\beta}_9$, the corresponding transformation angles are fixed by the renormalizability constraints as discussed in [11]. In all applications to nuclear forces and currents considered so far, the dependence on α_5 drops in the final results.

(1) Terms $\propto g_A^4 C_S$ and $g_A^4 C_T$:

$$\begin{aligned} V=\eta\Bigg[&-\frac{1}{2}H_{21}^{(1)}\frac{\lambda^1}{E_\pi}H_{21}^{(1)}\eta H_{21}^{(1)}\frac{\lambda^1}{E_\pi}H_{40}^{(2)}\frac{\lambda^1}{E_\pi^2}H_{21}^{(1)}-\frac{1}{2}H_{21}^{(1)}\frac{\lambda^1}{E_\pi}H_{21}^{(1)}\eta H_{21}^{(1)}\frac{\lambda^1}{E_\pi^2}H_{40}^{(2)}\frac{\lambda^1}{E_\pi}H_{21}^{(1)}\\ &-\frac{1}{2}H_{21}^{(1)}\frac{\lambda^1}{E_\pi^2}H_{21}^{(1)}\eta H_{21}^{(1)}\frac{\lambda^1}{E_\pi}H_{40}^{(2)}\frac{\lambda^1}{E_\pi}H_{21}^{(1)}-\frac{1}{2}H_{40}^{(2)}\eta H_{21}^{(1)}\frac{\lambda^1}{E_\pi}H_{21}^{(1)}\frac{\lambda^2}{E_\pi}H_{21}^{(1)}\frac{\lambda^1}{E_\pi^2}H_{21}^{(1)}\\ &-\frac{1}{2}H_{40}^{(2)}\eta H_{21}^{(1)}\frac{\lambda^1}{E_\pi}H_{21}^{(1)}\frac{\lambda^2}{E_\pi^2}H_{21}^{(1)}\frac{\lambda^1}{E_\pi}H_{21}^{(1)}-\frac{1}{2}H_{40}^{(2)}\eta H_{21}^{(1)}\frac{\lambda^1}{E_\pi^2}H_{21}^{(1)}\frac{\lambda^2}{E_\pi}H_{21}^{(1)}\frac{\lambda^1}{E_\pi}H_{21}^{(1)}\\ &+\frac{1}{2}H_{40}^{(2)}\eta H_{21}^{(1)}\frac{\lambda^1}{E_\pi}H_{21}^{(1)}\eta H_{21}^{(1)}\frac{\lambda^1}{E_\pi^3}H_{21}^{(1)}+\frac{3}{8}H_{40}^{(2)}\eta H_{21}^{(1)}\frac{\lambda^1}{E_\pi^2}H_{21}^{(1)}\eta H_{21}^{(1)}\frac{\lambda^1}{E_\pi^2}H_{21}^{(1)}\end{aligned}$$

$$
\begin{aligned}
&+\frac{1}{8}H_{21}^{(1)}\frac{\lambda^1}{E_\pi^2}H_{21}^{(1)}\eta H_{40}^{(2)}\eta H_{21}^{(1)}\frac{\lambda^1}{E_\pi^2}H_{21}^{(1)}+H_{21}^{(1)}\frac{\lambda^1}{E_\pi}H_{21}^{(1)}\frac{\lambda^2}{E_\pi}H_{21}^{(1)}\frac{\lambda^1}{E_\pi}H_{40}^{(2)}\frac{\lambda^1}{E_\pi}H_{21}^{(1)}\\
&+\frac{1}{2}H_{21}^{(1)}\frac{\lambda^1}{E_\pi}H_{21}^{(1)}\frac{\lambda^2}{E_\pi}H_{40}^{(2)}\frac{\lambda^2}{E_\pi}H_{21}^{(1)}\frac{\lambda^1}{E_\pi}H_{21}^{(1)}+H_{21}^{(1)}\frac{\lambda^1}{E_\pi}H_{21}^{(1)}\eta H_{21}^{(1)}\frac{\lambda^1}{E_\pi^3}H_{21}^{(1)}\eta H_{40}^{(2)}\\
&-\frac{1}{2}H_{21}^{(1)}\frac{\lambda^1}{E_\pi^3}H_{21}^{(1)}\eta H_{21}^{(1)}\frac{\lambda^1}{E_\pi}H_{21}^{(1)}\eta H_{40}^{(2)}-\frac{1}{4}H_{21}^{(1)}\frac{\lambda^1}{E_\pi}H_{21}^{(1)}\frac{\lambda^2}{E_\pi}H_{21}^{(1)}\frac{\lambda^1}{E_\pi^2}H_{21}^{(1)}\eta H_{40}^{(2)}\\
&+\frac{1}{4}H_{21}^{(1)}\frac{\lambda^1}{E_\pi^2}H_{21}^{(1)}\frac{\lambda^2}{E_\pi}H_{21}^{(1)}\frac{\lambda^1}{E_\pi}H_{21}^{(1)}\eta H_{40}^{(2)}\Bigg]\eta+\text{H.c.}
\end{aligned}
\tag{A1}
$$

(2) Terms $\propto g_A^2 C_S$ and $g_A^2 C_T$:

$$
\begin{aligned}
V=\eta\Bigg[&-2\alpha_5 H_{40}^{(2)}\eta H_{21}^{(1)}\frac{\lambda^1}{E_\pi}H_{21}^{(1)}\frac{\lambda^2}{E_\pi^2}H_{22}^{(2)}+\left(\frac{1}{2}+\alpha_5\right)H_{40}^{(2)}\eta H_{21}^{(1)}\frac{\lambda^1}{E_\pi}H_{22}^{(2)}\frac{\lambda^1}{E_\pi^2}H_{21}^{(1)}\\
&+\left(\frac{1}{2}+\alpha_5\right)H_{40}^{(2)}\eta H_{22}^{(2)}\frac{\lambda^2}{E_\pi}H_{21}^{(1)}\frac{\lambda^1}{E_\pi^2}H_{21}^{(1)}+\left(\frac{1}{2}-\alpha_5\right)H_{40}^{(2)}\eta H_{21}^{(1)}\frac{\lambda^1}{E_\pi^2}H_{21}^{(1)}\frac{\lambda^2}{E_\pi}H_{22}^{(2)}\\
&+\left(\frac{1}{2}-\alpha_5\right)H_{40}^{(2)}\eta H_{21}^{(1)}\frac{\lambda^1}{E_\pi^2}H_{22}^{(2)}\frac{\lambda^1}{E_\pi}H_{21}^{(1)}+(1+2\alpha_5)H_{40}^{(2)}\eta H_{22}^{(2)}\frac{\lambda^2}{E_\pi^2}H_{21}^{(1)}\frac{\lambda^1}{E_\pi}H_{21}^{(1)}\\
&-H_{21}^{(1)}\frac{\lambda^1}{E_\pi}H_{21}^{(1)}\frac{\lambda^2}{E_\pi}H_{40}^{(2)}\frac{\lambda^2}{E_\pi}H_{22}^{(2)}-H_{21}^{(1)}\frac{\lambda^1}{E_\pi}H_{22}^{(2)}\frac{\lambda^1}{E_\pi}H_{40}^{(2)}\frac{\lambda^1}{E_\pi}H_{21}^{(1)}\\
&-H_{21}^{(1)}\frac{\lambda^1}{E_\pi}H_{40}^{(2)}\frac{\lambda^1}{E_\pi}H_{21}^{(1)}\frac{\lambda^2}{E_\pi}H_{22}^{(2)}\Bigg]\eta+\text{H.c.}
\end{aligned}
\tag{A2}
$$

(3) Retardation corrections $\propto g_A^4/m$:

$$
\begin{aligned}
V=\eta\Bigg[&\left(\frac{1}{2}+\bar\beta_8\right)H_{21}^{(1)}\frac{\lambda^1}{E_\pi}H_{21}^{(1)}\eta H_{21}^{(1)}\frac{\lambda^1}{E_\pi^3}H_{21}^{(1)}\eta H_{20}^{(2)}-H_{21}^{(1)}\frac{\lambda^1}{E_\pi}H_{21}^{(1)}\eta H_{21}^{(1)}\frac{\lambda^1}{E_\pi^3}H_{20}^{(2)}\lambda^1 H_{21}^{(1)}\\
&+\left(\frac{1}{2}-\bar\beta_8\right)H_{21}^{(1)}\frac{\lambda^1}{E_\pi}H_{21}^{(1)}\eta H_{20}^{(2)}\eta H_{21}^{(1)}\frac{\lambda^1}{E_\pi^3}H_{21}^{(1)}-\frac{3}{4}H_{21}^{(1)}\frac{\lambda^1}{E_\pi}H_{21}^{(1)}\frac{\lambda^2}{E_\pi}H_{21}^{(1)}\frac{\lambda^1}{E_\pi^2}H_{21}^{(1)}\eta H_{20}^{(2)}\\
&+H_{21}^{(1)}\frac{\lambda^1}{E_\pi}H_{21}^{(1)}\frac{\lambda^2}{E_\pi}H_{21}^{(1)}\frac{\lambda^1}{E_\pi^2}H_{20}^{(2)}\lambda^1 H_{21}^{(1)}-\frac{1}{2}H_{21}^{(1)}\frac{\lambda^1}{E_\pi}H_{21}^{(1)}\frac{\lambda^2}{E_\pi^2}H_{21}^{(1)}\frac{\lambda^1}{E_\pi}H_{21}^{(1)}\eta H_{20}^{(2)}\\
&+\frac{1}{2}H_{21}^{(1)}\frac{\lambda^1}{E_\pi}H_{21}^{(1)}\frac{\lambda^2}{E_\pi^2}H_{20}^{(2)}\lambda^2 H_{21}^{(1)}\frac{\lambda^1}{E_\pi}H_{21}^{(1)}+\frac{3}{8}H_{21}^{(1)}\frac{\lambda^1}{E_\pi^2}H_{21}^{(1)}\eta H_{21}^{(1)}\frac{\lambda^1}{E_\pi^2}H_{21}^{(1)}\eta H_{20}^{(2)}\\
&-\frac{1}{2}H_{21}^{(1)}\frac{\lambda^1}{E_\pi^2}H_{21}^{(1)}\eta H_{21}^{(1)}\frac{\lambda^1}{E_\pi^2}H_{20}^{(2)}\lambda^1 H_{21}^{(1)}+\frac{1}{8}H_{21}^{(1)}\frac{\lambda^1}{E_\pi^2}H_{21}^{(1)}\eta H_{20}^{(2)}\eta H_{21}^{(1)}\frac{\lambda^1}{E_\pi^2}H_{21}^{(1)}\\
&-\frac{1}{4}H_{21}^{(1)}\frac{\lambda^1}{E_\pi^2}H_{21}^{(1)}\frac{\lambda^2}{E_\pi}H_{21}^{(1)}\frac{\lambda^1}{E_\pi^2}H_{21}^{(1)}\eta H_{20}^{(2)}\Bigg]\eta+\text{H.c.}
\end{aligned}
\tag{A3}
$$

(4) Retardation corrections $\propto g_A^2/m$:

$$
\begin{aligned}
V=\eta\Bigg[&(1+2\alpha_5)H_{21}^{(1)}\frac{\lambda^1}{E_\pi}H_{21}^{(1)}\frac{\lambda^2}{E_\pi^2}H_{22}^{(2)}\eta H_{20}^{(2)}-H_{21}^{(1)}\frac{\lambda^1}{E_\pi}H_{21}^{(1)}\frac{\lambda^2}{E_\pi^2}H_{20}^{(2)}\lambda^2 H_{22}^{(2)}\\
&+\frac{1}{2}(1-2\alpha_5)H_{21}^{(1)}\frac{\lambda^1}{E_\pi}H_{22}^{(2)}\frac{\lambda^1}{E_\pi^2}H_{21}^{(1)}\eta H_{20}^{(2)}-H_{21}^{(1)}\frac{\lambda^1}{E_\pi}H_{22}^{(2)}\frac{\lambda^1}{E_\pi^2}H_{20}^{(2)}\lambda^1 H_{21}^{(1)}\\
&+\frac{1}{2}(1+2\alpha_5)H_{21}^{(1)}\frac{\lambda^1}{E_\pi^2}H_{21}^{(1)}\frac{\lambda^2}{E_\pi}H_{22}^{(2)}\eta H_{20}^{(2)}+\frac{1}{2}(1+2\alpha_5)H_{21}^{(1)}\frac{\lambda^1}{E_\pi^2}H_{22}^{(2)}\frac{\lambda^1}{E_\pi}H_{21}^{(1)}\eta H_{20}^{(2)}\\
&-H_{21}^{(1)}\frac{\lambda^1}{E_\pi^2}H_{20}^{(2)}\lambda^1 H_{21}^{(1)}\frac{\lambda^2}{E_\pi}H_{22}^{(2)}-2\alpha_5 H_{22}^{(2)}\frac{\lambda^2}{E_\pi^2}H_{21}^{(1)}\frac{\lambda^1}{E_\pi}H_{21}^{(1)}\eta H_{20}^{(2)}\\
&+\frac{1}{2}(1-2\alpha_5)H_{22}^{(2)}\frac{\lambda^2}{E_\pi}H_{21}^{(1)}\frac{\lambda^1}{E_\pi^2}H_{21}^{(1)}\eta H_{20}^{(2)}-\frac{1}{2}H_{21}^{(1)}\frac{\lambda^1}{E_\pi^3}H_{21}^{(1)}\eta H_{20}^{(2)}\eta H_{20}^{(2)}\\
&+H_{21}^{(1)}\frac{\lambda^1}{E_\pi^3}H_{20}^{(2)}\lambda^1 H_{21}^{(1)}\eta H_{20}^{(2)}-\frac{1}{2}H_{21}^{(1)}\frac{\lambda^1}{E_\pi^3}H_{20}^{(2)}\lambda^1 H_{20}^{(2)}\lambda^1 H_{21}^{(1)}\Bigg]\eta+\text{H.c.}
\end{aligned}
\tag{A4}
$$

(5) Retardation corrections $\propto g_A^2 C_S/m$ and $g_A^2 C_T/m$:

$$V = \eta\left[\frac{1}{2}H_{21}^{(1)}\frac{\lambda^1}{E_\pi}H_{40}^{(2)}\frac{\lambda^1}{E_\pi^2}H_{21}^{(1)}\eta H_{20}^{(2)} - H_{21}^{(1)}\frac{\lambda^1}{E_\pi}H_{40}^{(2)}\frac{\lambda^1}{E_\pi^2}H_{20}^{(2)}\lambda^1 H_{21}^{(1)} + \frac{1}{2}H_{21}^{(1)}\frac{\lambda^1}{E_\pi^2}H_{40}^{(2)}\frac{\lambda^1}{E_\pi}H_{21}^{(1)}\eta H_{20}^{(2)}\right.$$
$$-\left(\frac{1}{2}-\bar{\beta}_8\right)H_{21}^{(1)}\frac{\lambda^1}{E_\pi^3}H_{21}^{(1)}\eta H_{20}^{(2)}\eta H_{40}^{(2)} + H_{21}^{(1)}\frac{\lambda^1}{E_\pi^3}H_{20}^{(2)}\lambda^1 H_{21}^{(1)}\eta H_{40}^{(2)}$$
$$\left.-\left(\frac{1}{2}+\bar{\beta}_8\right)H_{40}^{(2)}\eta H_{21}^{(1)}\frac{\lambda^1}{E_\pi^3}H_{21}^{(1)}\eta H_{20}^{(2)}\right]\eta + \text{H.c.} \tag{A5}$$

(6) Terms involving $1/m$ corrections to the g_A vertex, $\propto g_A^4/m$:

$$V = \eta\left[\left(\frac{1}{2}+\bar{\beta}_9\right)H_{21}^{(1)}\frac{\lambda^1}{E_\pi}H_{21}^{(1)}\eta H_{21}^{(1)}\frac{\lambda^1}{E_\pi^2}H_{21}^{(3)} + \left(\frac{1}{2}-\bar{\beta}_9\right)H_{21}^{(1)}\frac{\lambda^1}{E_\pi}H_{21}^{(1)}\eta H_{21}^{(3)}\frac{\lambda^1}{E_\pi^2}H_{21}^{(1)}\right.$$
$$-H_{21}^{(1)}\frac{\lambda^1}{E_\pi}H_{21}^{(1)}\frac{\lambda^2}{E_\pi}H_{21}^{(1)}\frac{\lambda^1}{E_\pi}H_{21}^{(3)} - H_{21}^{(1)}\frac{\lambda^1}{E_\pi}H_{21}^{(1)}\frac{\lambda^2}{E_\pi}H_{21}^{(3)}\frac{\lambda^1}{E_\pi}H_{21}^{(1)}$$
$$\left.+\frac{1}{2}H_{21}^{(1)}\frac{\lambda^1}{E_\pi^2}H_{21}^{(1)}\eta H_{21}^{(1)}\frac{\lambda^1}{E_\pi}H_{21}^{(3)} + \frac{1}{2}H_{21}^{(1)}\frac{\lambda^1}{E_\pi^2}H_{21}^{(1)}\eta H_{21}^{(3)}\frac{\lambda^1}{E_\pi}H_{21}^{(1)}\right]\eta + \text{H.c.} \tag{A6}$$

(7) Terms involving $1/m$ corrections to the g_A vertex, $\propto g_A^2 C_S/m$ and $g_A^2 C_T/m$:

$$V = \eta\left[H_{21}^{(1)}\frac{\lambda^1}{E_\pi}H_{40}^{(2)}\frac{\lambda^1}{E_\pi}H_{21}^{(3)} - \left(\frac{1}{2}-\bar{\beta}_9\right)H_{21}^{(1)}\frac{\lambda^1}{E_\pi^2}H_{21}^{(3)}\eta H_{40}^{(2)}\right.$$
$$\left.-\left(\frac{1}{2}+\bar{\beta}_9\right)H_{21}^{(3)}\frac{\lambda^1}{E_\pi^2}H_{21}^{(1)}\eta H_{40}^{(2)}\right]\eta + \text{H.c.} \tag{A7}$$

Here and in what follows, we adopt the notation of Refs. [4,11–13]. In particular, the subscripts a and b in $H_{ab}^{(\kappa)}$ refer to the number of the nucleon and pion fields, respectively, while the superscript κ gives the inverse mass dimension of the corresponding coupling constant;[7] see Ref. [11] for more details. The chiral order associated with a given contribution can easily be read off by adding together the dimensions κ of $H_{ab}^{(\kappa)}$. More precisely, it is given by $\sum_i \kappa_i - 2$. In the above equations, η (λ) denote projection operators onto the purely nucleonic (the remaining) part of the Fock space satisfying $\eta^2 = \eta, \lambda^2 = \lambda, \eta\lambda = \lambda\eta = 0$, and $\lambda + \eta = \mathbf{1}$. The superscript i of λ^i refers to the number of pions in the corresponding intermediate state. Furthermore, E_π denotes the total energy of the pions in the corresponding state, $E_\pi = \sum_i (\vec{l}_i^{\,2} + M_\pi^2)^{1/2}$, with $\vec{l}_i$ being the corresponding pion momenta.

APPENDIX B: COORDINATE-SPACE REPRESENTATION

In this appendix we give the coordinate-space representation of the obtained 3NF contributions. Here and in what follows, we adopt the notation of Refs. [4,11] and use the dimensionless profile functions $U_{1,2}$, W, and $W_{1,2}$ defined for a general form of a local regulator function F^Λ according to

$$U_1(x) = \frac{4\pi}{M_\pi}\int\frac{d^3q}{(2\pi)^3}\frac{e^{i\vec{q}\cdot\vec{x}/M_\pi}}{\vec{q}^{\,2}+M_\pi^2}F^\Lambda(q) \overset{\Lambda\to\infty}{\longrightarrow} \frac{e^{-x}}{x},$$
$$U_2(x) = 8\pi M_\pi\int\frac{d^3q}{(2\pi)^3}\frac{e^{i\vec{q}\cdot\vec{x}/M_\pi}}{\left(\vec{q}^{\,2}+M_\pi^2\right)^2}F^\Lambda(q) \overset{\Lambda\to\infty}{\longrightarrow} e^{-x},$$
$$W(x) = \frac{1}{M_\pi^3}\int\frac{d^3q}{(2\pi)^3}e^{i\vec{q}\cdot\vec{x}/M_\pi}F^\Lambda(q) \overset{\Lambda\to\infty}{\longrightarrow} \delta^3(x),$$
$$W_1(x) = \frac{4\pi}{M_\pi^2}\int\frac{d^3q}{(2\pi)^3}e^{i\vec{q}\cdot\vec{x}/M_\pi}A(q)F^\Lambda(q) \overset{\Lambda\to\infty}{\longrightarrow} \frac{e^{-2x}}{2x^2},$$
$$W_2(x) = \frac{4\pi}{M_\pi^4}\int\frac{d^3q}{(2\pi)^3}e^{i\vec{q}\cdot\vec{x}/M_\pi}q^2A(q)F^\Lambda(q) = -\nabla_x^2 W_1(x). \tag{B1}$$

For the two-pion-exchange-contact terms in Eqs. (3.1) and (3.5) we find

$$V_{2\pi\text{-cont}} = \frac{g_A^2 C_T M_\pi^7}{192\pi^2 F_\pi^4}\big[2\boldsymbol{\tau}_1\cdot\boldsymbol{\tau}_2(\vec{\sigma}_2\cdot\vec{\sigma}_3)$$
$$\times\left\{4\pi\left(3g_A^2-1\right)W(x_{12}) - 2g_A^2U_1(2x_{12})\right.$$
$$\left.+\left(2g_A^2-1\right)[2W_1(x_{12})+W_2(x_{12})]\right\}$$
$$-9g_A^2[(\vec{\sigma}_1\cdot\vec{\nabla}_{12})(\vec{\sigma}_2\cdot\vec{\nabla}_{12})W_1(x_{12})$$
$$+(\vec{\sigma}_1\cdot\vec{\sigma}_2)W_2(x_{12})]\big]W(x_{32}) + 5\text{ permutations}. \tag{B2}$$

[7] For $1/m$ corrections, κ_i corresponds to the inverse power of coupling constants plus twice the power of m^{-1}. In particular, $\kappa = 2$ for the nucleon kinetic energy term H_{20}.

Next, the coordinate-space representation of the relativistic corrections to the two-pion exchange 3NF emerges from taking the Fourier transform of Eq. (4.9):

$$V_{2\pi,1/m} = \frac{g_A^2 M_\pi^6}{1024 m \pi^2 F_\pi^4} (\boldsymbol{\tau}_1 \cdot \boldsymbol{\tau}_3 \tilde{A}_{123} + [\boldsymbol{\tau}_1 \times \boldsymbol{\tau}_2] \cdot \boldsymbol{\tau}_3 \tilde{B}_{123}) + 5 \text{ permutations}, \tag{B3}$$

where

$$\begin{aligned} \tilde{A}_{123} &= (\vec{\sigma}_1 \cdot \vec{\nabla}_{12})(\vec{\sigma}_3 \cdot \vec{\nabla}_{32}) \tilde{a}_{123} + \left\{ \left(\vec{\sigma}_3 \cdot \frac{\vec{p}_3}{M_\pi} \right), (\vec{\sigma}_1 \cdot \vec{\nabla}_{12}) \tilde{c}_{123} \right\}, \\ \tilde{B}_{123} &= (\vec{\sigma}_1 \cdot \vec{\nabla}_{12})(\vec{\sigma}_3 \cdot \vec{\nabla}_{32}) \tilde{b}_{123} + \left\{ \left(\vec{\sigma}_3 \cdot \frac{\vec{p}_3}{M_\pi} \right), (\vec{\sigma}_1 \cdot \vec{\nabla}_{12}) \tilde{d}_{123} \right\}, \end{aligned} \tag{B4}$$

and the functions $\tilde{a}_{123}$, $\tilde{b}_{123}$, $\tilde{c}_{123}$, and $\tilde{d}_{123}$ are given by

$$\begin{aligned} \tilde{a}_{123} &= g_A^2 (1 - 2\bar{\beta}_8)(\vec{\nabla}_{12} \cdot \vec{\nabla}_{32})^2 U_2(x_{12}) U_1(x_{32}) + g_A^2 \left\{ (1 - 2\bar{\beta}_8) \frac{\vec{p}_2}{M_\pi} + (1 + 2\bar{\beta}_8) \frac{\vec{p}_1}{M_\pi}, \vec{\nabla}_{12} [\vec{\nabla}_{12} \times \vec{\nabla}_{32}] \cdot \vec{\sigma}_2 U_2(x_{12}) U_1(x_{32}) \right\} \\ &\quad - 2 g_A^2 (2\bar{\beta}_9 - 1) \nabla_{12}^2 U_1(x_{12}) U_1(x_{32}) + 2 g_A^2 (2\bar{\beta}_9 - 1) \left\{ \frac{\vec{p}_2}{M_\pi}, [\vec{\sigma}_2 \times \vec{\nabla}_{12}] U_1(x_{12}) U_1(x_{32}) \right\}, \\ \tilde{c}_{123} &= -2 g_A^2 (2\bar{\beta}_9 + 1) [\vec{\nabla}_{12} \times \vec{\nabla}_{32}] \cdot \vec{\sigma}_2 U_1(x_{12}) U_1(x_{32}), \\ \tilde{b}_{123} &= g_A^2 (1 - 2\bar{\beta}_8) [\vec{\nabla}_{12} \times \vec{\nabla}_{32}] \cdot \vec{\sigma}_2 (\vec{\nabla}_{12} \cdot \vec{\nabla}_{32}) U_2(x_{12}) U_1(x_{32}) \\ &\quad - g_A^2 \left\{ (1 - 2\bar{\beta}_8) \frac{\vec{p}_2}{M_\pi} + (1 + 2\bar{\beta}_8) \frac{\vec{p}_1}{M_\pi}, \vec{\nabla}_{12} (\vec{\nabla}_{12} \cdot \vec{\nabla}_{32}) U_2(x_{12}) U_1(x_{32}) \right\} - 2 \left\{ \frac{\vec{p}_3}{M_\pi} - \frac{\vec{p}_2}{M_\pi}, \vec{\nabla}_{32} U_1(x_{12}) U_1(x_{32}) \right\} \\ &\quad - 2 g_A^2 (2\bar{\beta}_9 - 1) \left\{ \frac{\vec{p}_2}{M_\pi}, \vec{\nabla}_{12} U_1(x_{12}) U_1(x_{32}) \right\} - 2 [\vec{\nabla}_{12} \times \vec{\nabla}_{32}] \cdot \vec{\sigma}_2 U_1(x_{12}) U_1(x_{32}), \\ \tilde{d}_{123} &= 2 g_A^2 (2\bar{\beta}_9 + 1) (\vec{\nabla}_{12} \cdot \vec{\nabla}_{32}) U_1(x_{12}) U_1(x_{32}), \end{aligned} \tag{B5}$$

where $\vec{x}_{ij} \equiv M_\pi \vec{r}_{ij}$, $x_{ij} \equiv |\vec{x}_{ij}|$, and $\vec{r}_{ij} = \vec{r}_i - \vec{r}_j$ is the distance between the nucleons i and j. Furthermore, the $\vec{\nabla}_{ij}$ act on $\vec{x}_{ij}$ (i.e., are dimensionless) and $\vec{p}_i$ refer to the momentum operator of the nucleon i. Curly brackets denote, as usual, the anticommutator of two operators, $\{X, Y\} \equiv XY + YX$, and $\{\vec{X}, \vec{Y}\} \equiv \vec{X} \cdot \vec{Y} + \vec{Y} \cdot \vec{X}$.

Finally, the $1/m$ corrections to the one-pion-exchange-contact topology have the form

$$V_{1\pi\text{-cont},1/m} = \frac{g_A^2 M_\pi^6}{64 m \pi F_\pi^2} \boldsymbol{\tau}_1 \cdot \boldsymbol{\tau}_2 \left[(\vec{\sigma}_1 \cdot \vec{\nabla}_{12}) \tilde{f}_{123} + \left\{ \vec{\sigma}_1 \cdot \frac{\vec{p}_1}{M_\pi}, \tilde{g}_{123} \right\} \right] + 5 \text{ permutations}, \tag{B6}$$

with the functions $\tilde{f}_{123}$ and $\tilde{g}_{123}$ given by

$$\begin{aligned} \tilde{f}_{123} &= (1 - 2\bar{\beta}_8)(\vec{\nabla}_{12} \cdot \vec{\nabla}_{32}) \left[C_S (\vec{\nabla}_{12} \cdot \vec{\sigma}_2) + C_T (\vec{\nabla}_{12} \cdot \vec{\sigma}_3) \right] U_2(x_{12}) W(x_{32}) \\ &\quad - C_T \left\{ (1 - 2\bar{\beta}_8) \frac{\vec{p}_2}{M_\pi} + (1 + 2\bar{\beta}_8) \frac{\vec{p}_1}{M_\pi}, \vec{\nabla}_{12} \vec{\nabla}_{12} \cdot [\vec{\sigma}_2 \times \vec{\sigma}_3] U_2(x_{12}) W(x_{32}) \right\} \\ &\quad - 2(2\bar{\beta}_9 - 1) \left[C_S (\vec{\nabla}_{32} \cdot \vec{\sigma}_2) + C_T (\vec{\nabla}_{32} \cdot \vec{\sigma}_3) \right] U_1(x_{12}) W(x_{32}) \\ &\quad + 2 C_T (2\bar{\beta}_9 - 1) \left\{ \frac{\vec{p}_2}{M_\pi}, [\vec{\sigma}_2 \times \vec{\sigma}_3] U_1(x_{12}) W(x_{32}) \right\}, \\ \tilde{g}_{123} &= -2 C_T (2\bar{\beta}_9 + 1) \vec{\nabla}_{12} \cdot [\vec{\sigma}_2 \times \vec{\sigma}_3] U_1(x_{12}) W(x_{32}). \end{aligned} \tag{B7}$$

[1] E. Epelbaum, H. -W. Hammer, and Ulf-G. Meißner, Rev. Mod. Phys. **81**, 1773 (2009).

[2] R. Machleidt and D. R. Entem, Phys. Rept. **503**, 1 (2011).

[3] N. Kalantar-Nayestanaki, E. Epelbaum, J. G. Messchendorp, and A. Nogga, arXiv:1108.1227.

[4] V. Bernard, E. Epelbaum, H. Krebs, and Ulf-G. Meißner, Phys. Rev. C **77**, 064004 (2008).

[5] S. Ishikawa and M. R. Robilotta, Phys. Rev. C **76**, 014006 (2007).

[6] R. Skibinski, J. Golak, K. Topolnicki, H. Witala, E. Epelbaum, W. Glöckle, H. Krebs, and A. Nogga *et al.*, arXiv:1107.5163.

[7] E. Epelbaum, W. Glöckle, and Ulf-G. Meißner, Nucl. Phys. A **637**, 107 (1998).
[8] E. Epelbaum, W. Glöckle, and Ulf-G. Meißner, Nucl. Phys. A **671**, 295 (2000).
[9] E. Epelbaum, Ulf-G. Meißner, and W. Glöckle, Nucl. Phys. A **714**, 535 (2003).
[10] E. Epelbaum, W. Glöckle, and Ulf-G. Meißner, Nucl. Phys. A **747**, 362 (2005).
[11] E. Epelbaum, Eur. Phys. J. A **34**, 197 (2007).
[12] S. Kölling, E. Epelbaum, H. Krebs, and Ulf-G. Meißner, Phys. Rev. C **80**, 045502 (2009).
[13] S. Kölling, E. Epelbaum, H. Krebs, and Ulf-G. Meißner, arXiv:1107.0602.
[14] I. S. Gerstein, R. Jackiw, S. Weinberg, and B. W. Lee, Phys. Rev. D **3**, 2486 (1971).
[15] E. Epelbaum, Prog. Part. Nucl. Phys. **57**, 654 (2006).
[16] S. Weinberg, Phys. Lett. B **251**, 288 (1990).
[17] U. van Kolck, Phys. Rev. C **49**, 2932 (1994).
[18] E. Epelbaum and Ulf-G. Meißner, Phys. Rev. C **72**, 044001 (2005).
[19] V. Bernard, N. Kaiser, and Ulf-G. Meißner, Int. J. Mod. Phys. E **4**, 193 (1995).
[20] J. L. Friar, Phys. Rev. C **60**, 034002 (1999).
[21] L. Girlanda, S. Pastore, R. Schiavilla, and M. Viviani, Phys. Rev. C **81**, 034005 (2010).
[22] J. L. Friar and S. A. Coon, Phys. Rev. C **49**, 1272 (1994).